CFD Letters www.cfdl.issres.net Vol. 1 (1) – July 2009

Prediction of Lift and Drag Coefficients on Stationary Capsule in Pipeline

Mohamed F. Khalil [1] , Sadek Z. Kassab [1,2], Ihab G. Adam [1], and Mohamed A. Samaha [1C]
[1] *Mechanical Engineering Department, Faculty of Engineering Alexandria University, EGYPT*
[2] *Arab Academy for Science and Technology and Maritime Transport, Alexandria, EGYPT*

Received: 17/07/2009 – Revised 24/07/2009 – Accepted 29/07/2009

Abstract

The present study is primarily concerned with modeling 3D, steady, and turbulent flow over a stationary capsule in a pipeline to predict the pressure distribution around the capsule. The results were used to determine the lift and Drag on the capsule. The results were compared with the available published experimental data to validate the models. Two types of the two equation turbulence models ($k-\varepsilon$ and $k-\omega$) and a second moment closure model (Reynolds stress model *RSM*) were used in the numerical simulation to predict the results. The experimental data obtained for drag were shown to be in a good agreement with the three turbulence models. Whereas for lift estimation, only the RSM model compared well with the experimental data. This explains the limitation of using the two equation models.

Keywords: Capsule pipeline; Turbulence modeling; Lift; Drag; Eccentric Stationary Capsule.

1. Introduction

Hydraulic capsule pipeline (HCP) is an emerging technology by which freight is transported in capsules (cylindrical containers) suspended by a liquid, usually water, moving through a pipeline. Compared to conventional freight transportation modes such as truck and rail, HCP has several potential advantages: It is less energy-intensive [1], less harmful to environment, less labor-intensive (more automatic), Less subject to theft, less dependent on weather, more reliable, much safer to humans and animals, and in many circumstances more economical [2-3]. For these reasons, it is anticipated that HCP will play an essential role in freight transport in the 21st century [4-5] presented an overview, general theoretical and experimental analysis for capsule flow in a pipeline. Liu [6] presented an overview on the hydraulic capsule pipeline to introduce the basic concept of HCP. Liu and Graze [7] performed an experimental model analysis for stationary capsule in pipe to determine the lift and drag exerted on the capsule. Liu and Richards [8] studied the behavior of capsule correctly during startup or restart. An extension for the work of Liu and Richards was done in [9]. An Overview on freight pipelines: current status and anticipated future use was done in [10-11].

[C] Corresponding author: Mohamed A. Samaha
Email: moh_samaha@yahoo.com
© 2009-2012 All rights reserved. ISSR Journals

Turbulence modeling has been an area of intensive research for the last few decades. Hanjalic et al [12] described modeling strategies for turbulent wall flows subjected to strong pressure variations. Huang [13] discussed some Physical and computational aspects of flows with adverse pressure gradients. Kim et al [14] presented a computational model of complex turbulent flows using the Commercial Code FLUENT. Wilcox text [15] is regarded as one of the most comprehensive literature on turbulence modeling, in which the definition of the closure problem of turbulence, the models classification, and their properties are very well described. Ferziger and Peric [16] also explained many turbulence models.

As described in [10-11], the motion of capsules in pipe can be classified into four regimes as shown in Figure 1. In Regime 1, the bulk fluid velocity is so low that insufficient drag is developed on the capsules to overcome the contact friction between them and the pipe in order for them to move. Regime 2 starts when the velocity of the fluid is high enough to cause the capsules to slide along the pipe. However, the fluid velocity in Regime 2 is still relatively low, the contact friction between the capsules and the pipe is high, and the capsule velocity is less than the fluid velocity. Further increase in fluid velocity beyond those in Regime 2 causes the flow to enter Regime 3, in which the capsule velocity overtakes the fluid velocity. Regime 3 ends when the fluid velocity is so high that the capsules are lifted off the pipe wall and become waterborne. Thereafter, the flow enters Regime 4.

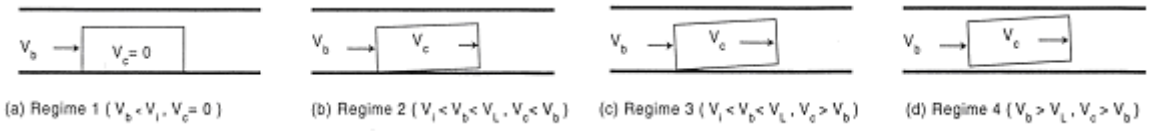

Figure 1. Four regimes of Hydraulic Capsule Pipeline flow [10-11]

Because of the importance of the hydraulic capsule pipeline in the application of the transportation, a research program concerning this type of transportation mode has been started at the Mechanical Engineering Department, Alexandria University in cooperation with others since 2002 first as an undergraduate B.Sc. project and proceeds as a graduate research. At the beginning of this research program, Khalil and Hammoud [17] provided an experimental investigation of the HCP with drag reducing surfactant to study its effect on the system performance. In addition, Khalil and Hammoud [18] provided an experimental analysis of the effect of the upward and downward inclination of the pipe on the flow properties. The second stage of the program, Khalil et al [19] established a numerical laminar annular flow model around a moving core in a pipe. As a continuation of this program, Khalil et al [20] developed a turbulent flow model to simulate the flow around a lifted off concentric long capsule as two and three dimensional flow in annulus between concentric long capsule and pipe. Furthermore, Khalil et al [21] modified the turbulent flow model to simulate the flow around concentric capsule train which consists of 12 short capsules arranged in this train. More details are given by Samaha [22]. As a continuation of this research program, the present study aims to model the turbulent flow by using $k-\varepsilon$, $k-\omega$ and RSM models around the stationary capsule (as shown in figure 2) by using the Commercial Software FLUENT to obtain the drag and lift coefficients and compare them with that obtained experimentally in [7].

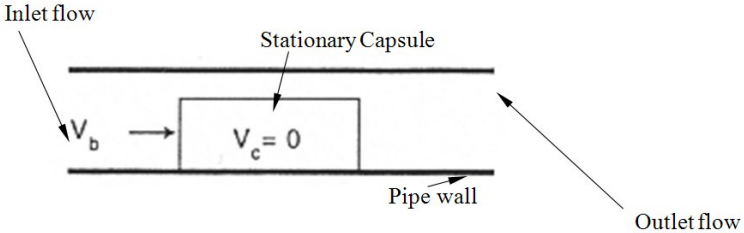

Figure 2. Schematic illustration of single stationary capsule in pipe.

2. Numerical details

2.1. Grid Generation and Meshing

The case study with its dimensions is shown in figure 3. A Hex/Wedge-Cooper unstructured mesh for the flow around the stationary capsule inside the pipe has been generated. The flow has complex structures including the three -dimensional flow separation and vortices after the capsule front and at the inlet to the annulus (at capsule tail).

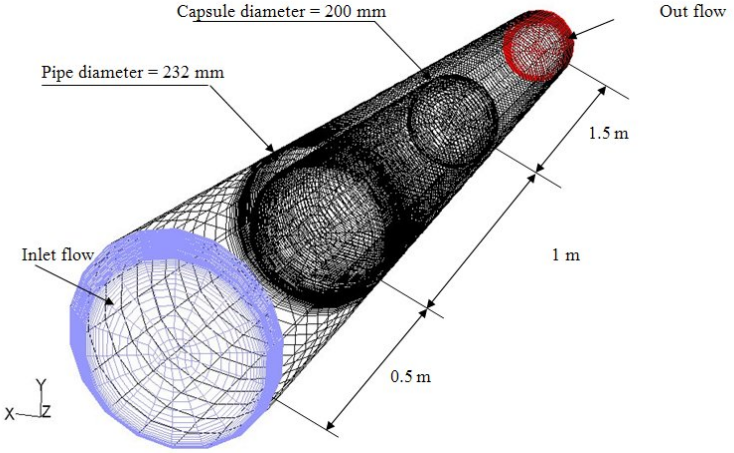

Figure 3. Viscous Hex/Wedge-Cooper mesh for a fully eccentric capsule in a pipe.

2.2. Governing equations

2.2.1. The Reynolds Averaged Equations of Motion

The case solved in the present study is turbulent, three dimensional, steady, incompressible, and constant property flow so that the Reynolds averaged Navier-Stokes equation (RANS) in the indicial notion form will be:

$$\rho \frac{\partial U_i}{\partial t} + \rho U_j \frac{\partial U_i}{\partial x_j} = -\frac{\partial P}{\partial x_i} + \frac{\partial}{\partial x_j}\left(2\mu S_{ji} - \rho \overline{u_j' u_i'}\right) \quad (1)$$

where

$$S_{ij} = \frac{1}{2}\left(\frac{\partial U_i}{\partial x_j} + \frac{\partial U_j}{\partial x_i}\right) \quad (2)$$

$\tau_{ij} = -\rho \overline{u_j' u_i'}$ is called Reynolds stress tensor which needs to be modelled by using a type of turbulence models. U_i, U_j are the velocities in the indicial notion form.

The continuity equation for the 3D-Incompressible flow is $\frac{\partial U_i}{\partial x_i} = 0$ (3)

2.2.2. Turbulence Modeling

The Reynolds-averaged approach to turbulence modeling requires that the Reynolds stresses in Equation 1 be appropriately modeled. A common method employs the Boussinesq hypothesis to relate the Reynolds stresses to the mean velocity gradients:

$$-\rho \overline{u_i' u_j'} = \mu_t \left(\frac{\partial u_i}{\partial x_j} + \frac{\partial u_j}{\partial x_i}\right) - \frac{2}{3}\left(\rho k + \mu_t \frac{\partial u_i}{\partial x_i}\right)\delta_{ij} \quad (4)$$

The Boussinesq hypothesis is used in the $k-\varepsilon$ and $k-\omega$ models. The disadvantage of the Boussinesq hypothesis as presented is that it assumes μ_t is an isotropic scalar quantity, which is not strictly true.

2.2.2.1 The Standard k-ε Model

It was proposed by Launder and Spalding [23] (equations from 5 to 8).

- Turbulent viscosity

$$\mu_t = \rho C_\mu k^2 / \varepsilon \tag{5}$$

- Turbulence kinetic energy

$$\frac{\partial k}{\partial t} + U_j \frac{\partial k}{\partial x_j} = \tau_{ij} \frac{\partial U_i}{\partial x_j} - \varepsilon + \frac{\partial}{\partial x_j}\left[\left(\nu + \nu_t / \sigma_k \right) \frac{\partial k}{\partial x_j} \right] \tag{6}$$

- Dissipation rate

$$\frac{\partial \varepsilon}{\partial t} + U_j \frac{\partial \varepsilon}{\partial x_j} = C_{\varepsilon 1} \frac{\varepsilon}{k} \tau_{ij} \frac{\partial U_i}{\partial x_j} - C_{\varepsilon 2} \frac{\varepsilon^2}{k} + \frac{\partial}{\partial x_j}\left[\left(\nu + \nu_t / \sigma_\varepsilon \right) \frac{\partial \varepsilon}{\partial x_j} \right] \tag{7}$$

Closure Coefficients and auxiliary relations

$C_{\varepsilon 1} = 1.44 \quad C_{\varepsilon 2} = 1.92 \quad C_\mu = 0.09 \quad \sigma_k = 1.0 \quad \sigma_\varepsilon = 1.3$ (Wilcox [15]) (8)

2.2.2.2 The Standard k-ω Model

This model is based on the Wilcox k-ω model [15] (equations from 9 to 15).

- Turbulent viscosity

$$\mu_t = \rho k / \omega \tag{9}$$

- Turbulence kinetic energy

$$\frac{\partial k}{\partial t} + U_j \frac{\partial k}{\partial x_j} = \tau_{ij} \frac{\partial U_i}{\partial x_j} - \beta^* k\omega + \frac{\partial}{\partial x_j}\left[\left(\nu + \sigma^* \nu_t \right) \frac{\partial k}{\partial x_j} \right] \tag{10}$$

- Specific dissipation rate

$$\frac{\partial \omega}{\partial t} + U_j \frac{\partial \omega}{\partial x_j} = \alpha \frac{\omega}{k} \tau_{ij} \frac{\partial U_i}{\partial x_j} - \beta \omega^2 + \frac{\partial}{\partial x_j}\left[\left(\nu + \sigma \nu_t \right) \frac{\partial \omega}{\partial x_j} \right] \tag{11}$$

Closure Coefficients and auxiliary relations:

$\alpha = 13/25 \quad \beta = \beta_o f_\beta \quad \beta^* = \beta_o^* f_{\beta^*} \quad \sigma = 1/2 \quad \sigma^* = 1/2$ (12)

$$\beta_o = 9/125 \qquad f_\beta = \frac{1 + 70 x_\omega}{1 + 80 x_\omega} \qquad x_\omega \equiv \left| \frac{\Omega_{ij} \Omega_{jk} S_{ki}}{\left(\beta_o^* \omega \right)^3} \right| \qquad \Omega_{ij} \frac{1}{2}\left(\frac{\partial U_i}{\partial x_j} - \frac{\partial U_j}{\partial x_i} \right) \tag{13}$$

$$\beta_o^* = 9/100 \qquad f_{\beta^*} = \begin{cases} 1 & x_k \le 0 \\ \frac{1 + 680\, x_k^2}{1 + 400\, x_k^2} & x_k > 0 \end{cases} \tag{14}$$

$$x_k \equiv \frac{1}{\omega^3}\left(\frac{\partial k}{\partial x_j} \frac{\partial \omega}{\partial x_j} \right) \qquad \varepsilon = \beta^* \omega k \quad \text{and} \quad \ell = \sqrt{k} / \omega \tag{15}$$

2.2.2.3 The Reynolds Stress Model (RSM)

Abandoning the isotropic eddy-viscosity hypothesis, the RSM closes the Reynolds-averaged Navier-Stokes equations by solving transport equations for the Reynolds stresses, together with an equation for the dissipation rate. This means that seven additional transport equations must be solved in three dimensional. Since the RSM accounts for the effects of streamline curvature, swirl, rotation, and rapid

changes in strain rate in a more rigorous manner than one-equation and two-equation models, it has greater potential to give accurate predictions for complex flows. However, the fidelity of RSM predictions is still limited by the closure assumptions employed to model various terms in the exact transport equations for the Reynolds stresses.

3. Results and discussion

Figure 4 shows the non-dimensional pressure head distribution along the stationary capsule in pipe at different orientation of capsule obtained by using the three different turbulence models. These figures shed some lights on how the lift and drag are developed on the capsule. Of course, the lift is developed by the difference of the integration of pressure distribution around the lower half of capsule area (i.e. at angles more that 90º) and that around the upper half of capsule area (i.e. at angles lower than 90º). On the other hand, the drag is developed from the pressure drop across the capsule length. The results of the pressure distribution around the stationary capsule in the pipe obtained by using the three different models are compared against the experimental data of Liu and Graze [7]. The models are run at the practical Reynolds number of 64194 in pipe and of 34560 in annulus. Figure 5 shows the comparison between the measured dimensionless pressure distribution and the numerically predicted one for different capsule orientations, θ, using the Standard k-ε Model. Also Figure 6 shows that by using the Standard k-ω Model and Figure 7 shows that by using the RSM model.

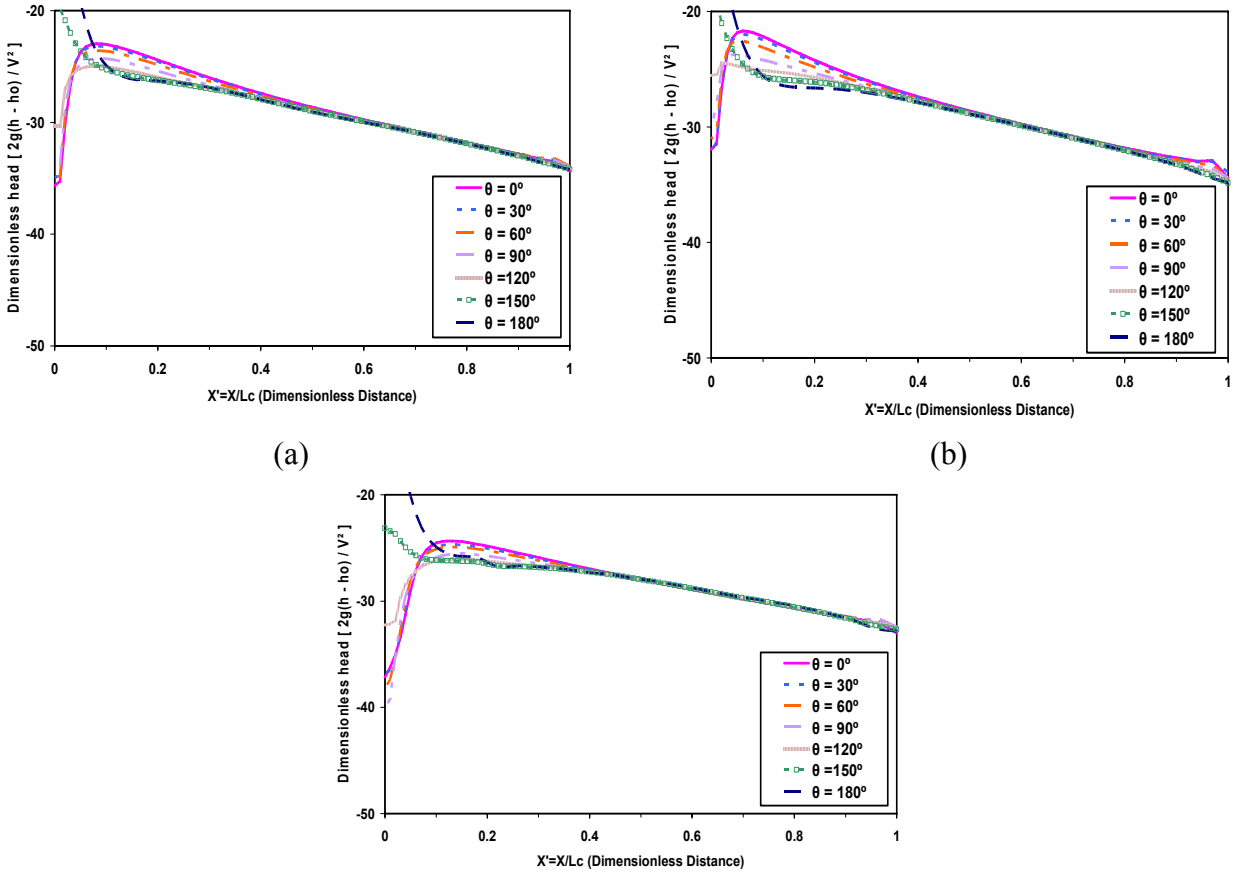

Figure 4. The non-dimensional pressure head distribution along the stationary capsule in pipe at different orientation of capsule obtained by using the three different turbulence models: (a) k-ε model, (b) k-ω model, (c) RSM model

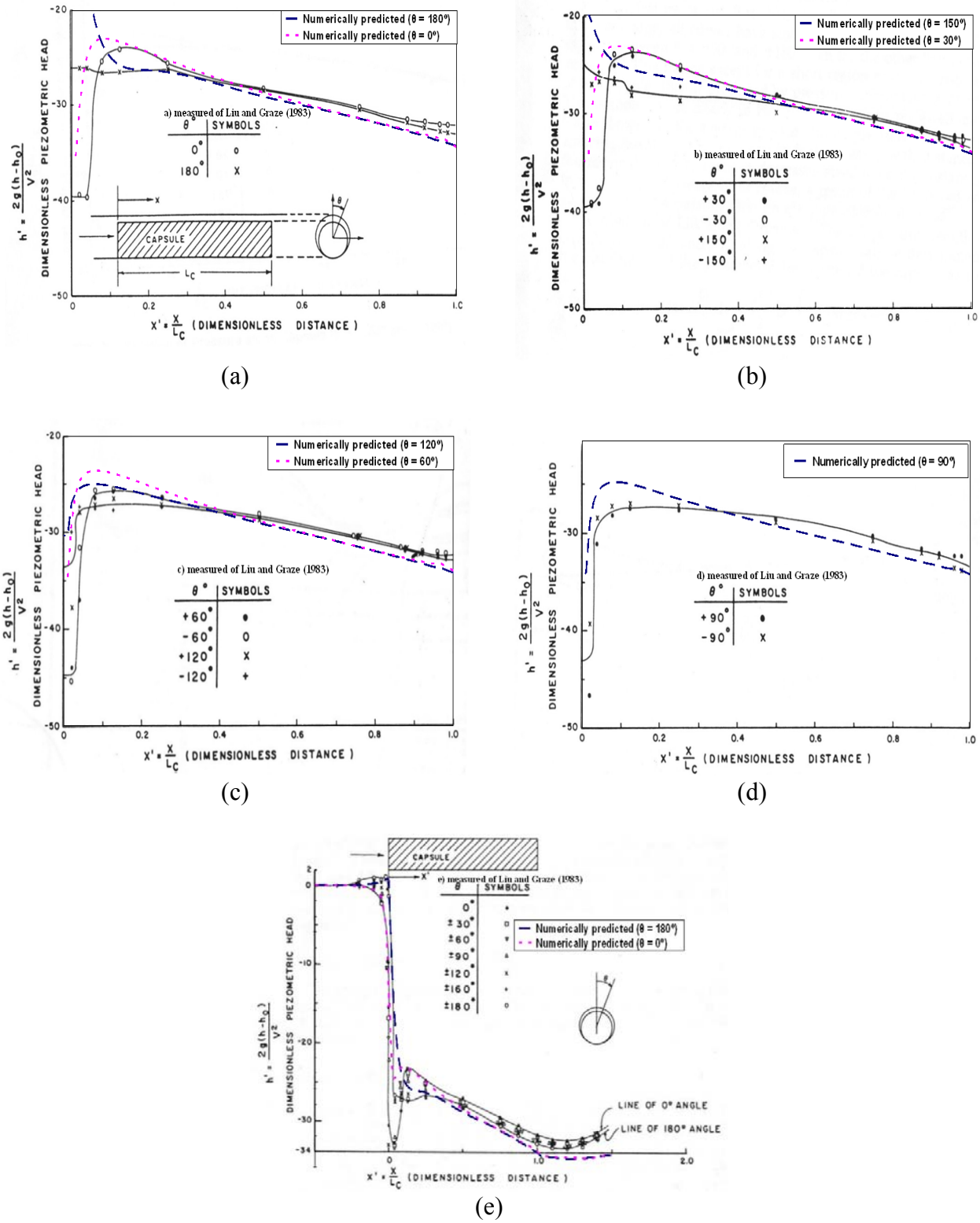

Figure 5. Comparison between the measured dimensionless pressure distribution by Liu and Graze [7] and the numerically predicted one for different capsule orientations by using the Standard k-ε Model: (a) θ = 0º and 180º, (b) 30º and 150º, (c) 60º and 120º, (d) 90º, (e) The pressure distribution along the pipe.

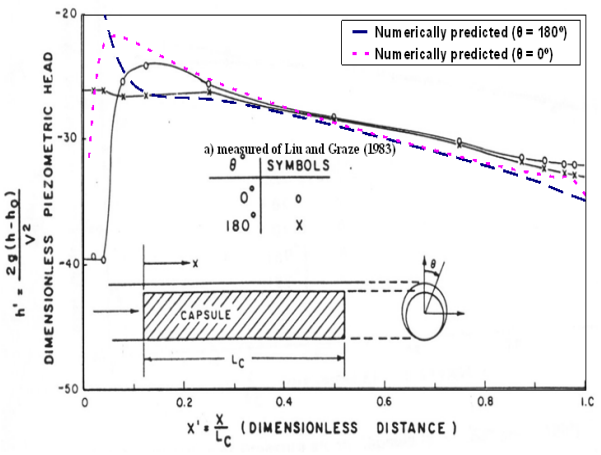

(a)

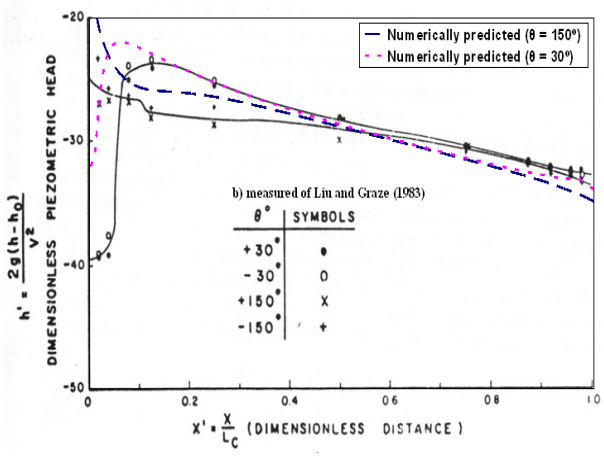

(b)

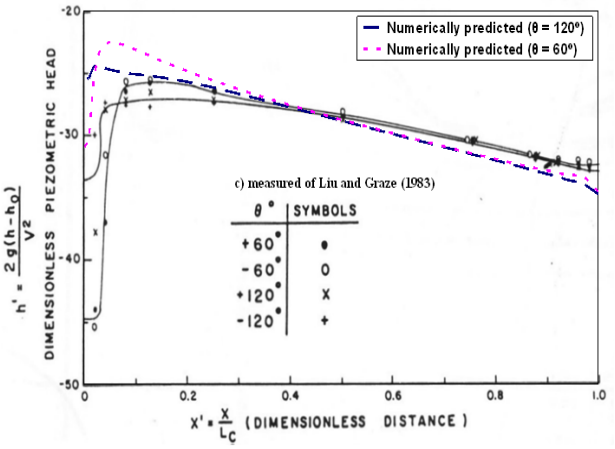

(c)

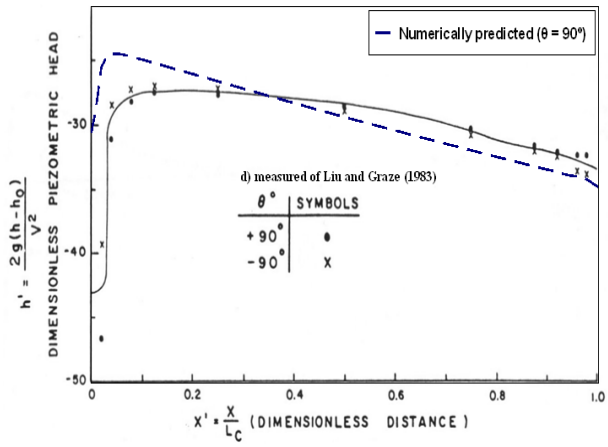

(d)

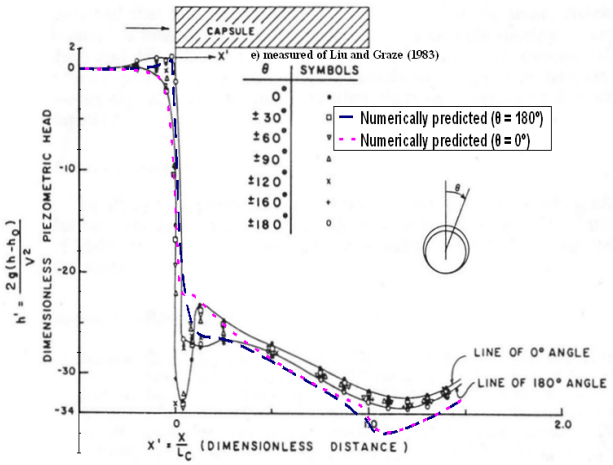

(e)

Figure 6. Comparison between the measured dimensionless pressure distribution by Liu and Graze [7] and the numerically predicted one for different capsule orientations by using the Standard k-ω Model: (a) θ = 0º and 180º, (b) 30º and 150º, (c) 60º and 120º, (d) 90º, (e) The pressure distribution along the pipe.

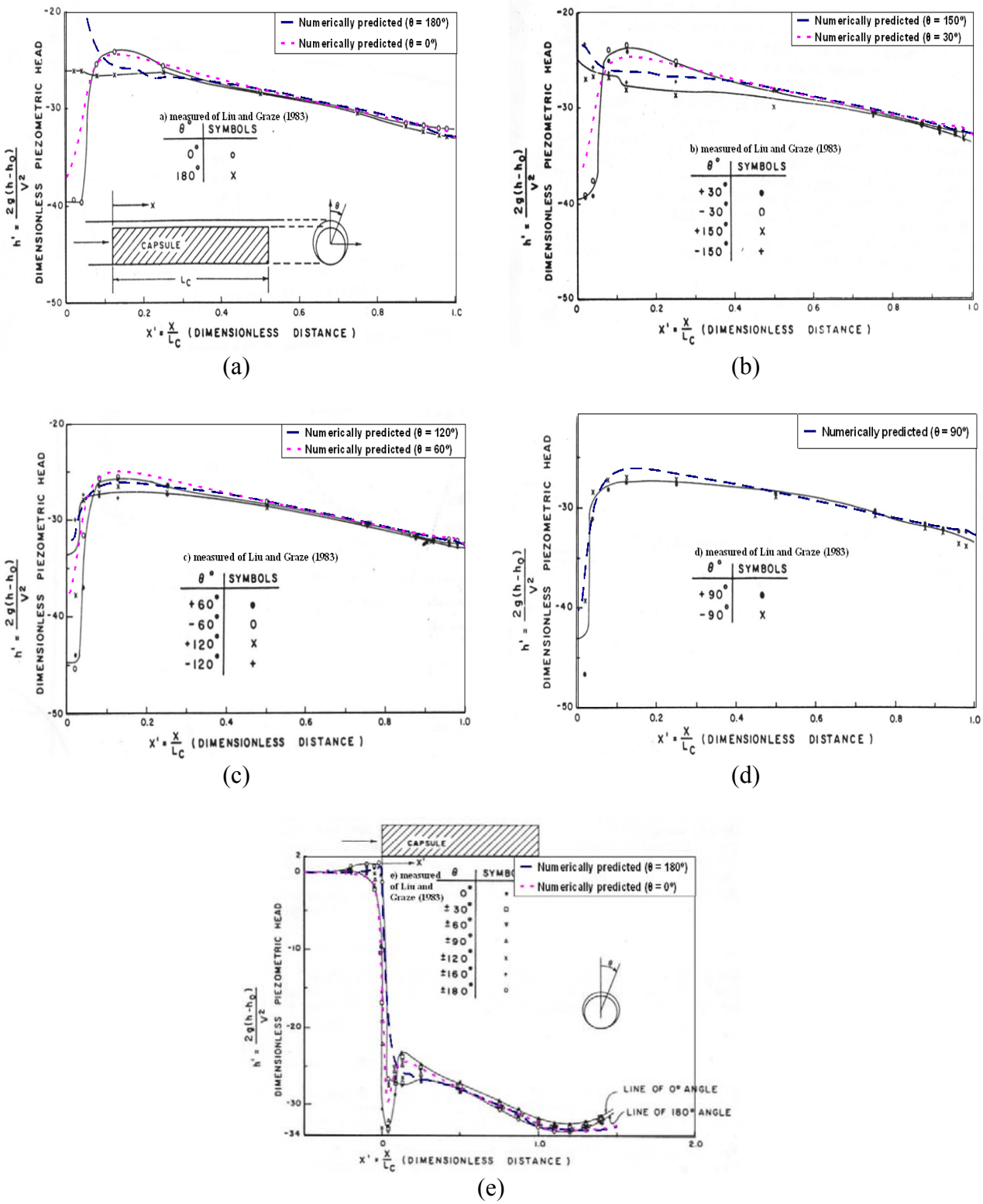

Figure 7. Comparison between the measured dimensionless pressure distribution by Liu and Graze [7] and the numerically predicted one for different capsule orientations by using the RSM Model: (a) θ = 0º and 180º, (b) 30º and 150º, (c) 60º and 120º, (d) 90º, (e) The pressure distribution along the pipe.

From figures 5, 6 and 7, it is obvious that the pressure suddenly decreases when the flow is subjected to sudden contraction from the pipe area to the annulus area. Moreover, as shown in figure 8 a large suction area exists near the upstream top of the capsule which is generated by the flow separation near the upstream edge of the capsule. The rapid increase in pressure indicates that the separation zone has reached a maximum height and the stream lines above the separation zone are starting to diverge after this point. Hence, the mean pressure gradient in this case is changed from favorable to unfavorable to favorable again.

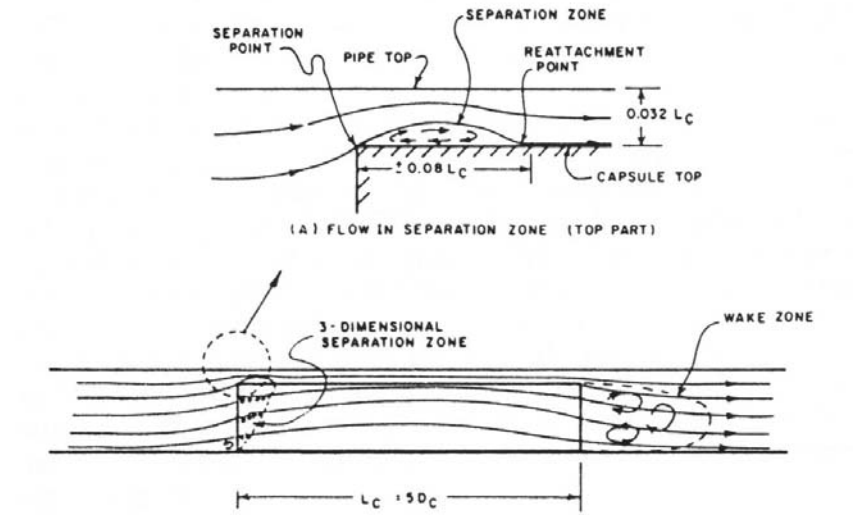

(a)

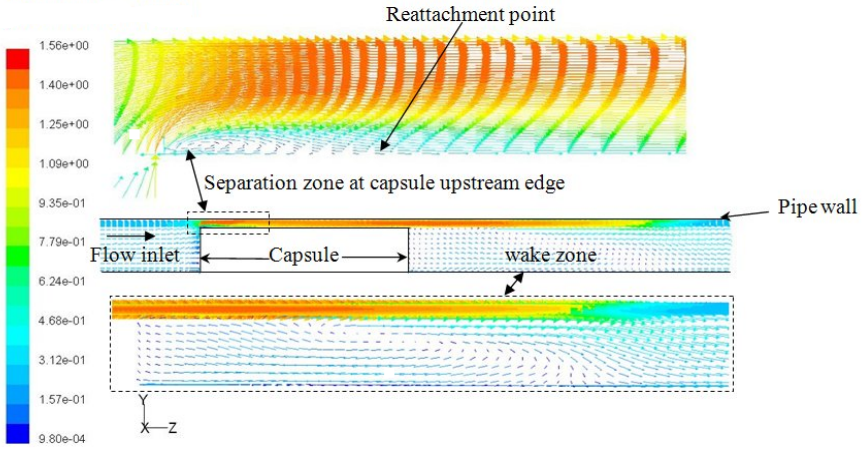

(b)

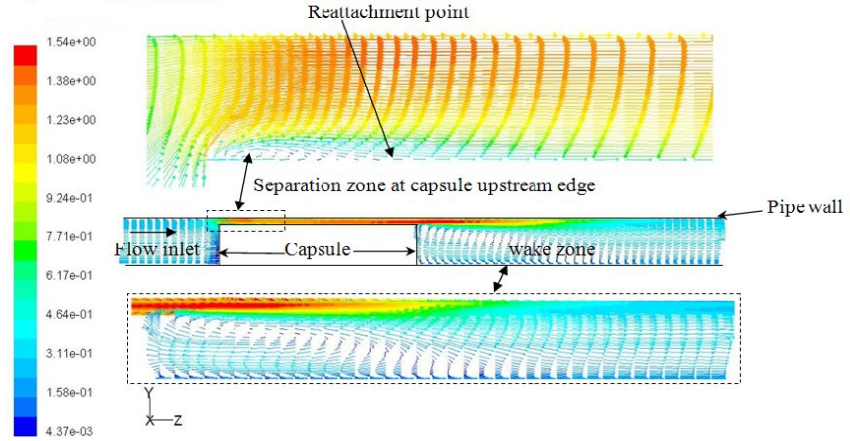

(c)

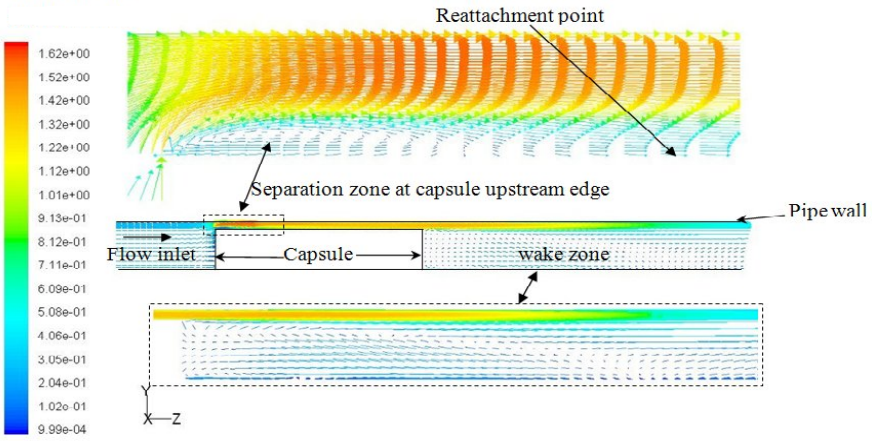

(d)

Figure 8. Flow pattern around stationary capsule (velocity vector in m/s) (a) Measured data from [7], (b) Standard k-ε Model, (c) Standard k-ω Model, (d) RSM model.

Table 1 shows comparison of numerically predicted lift and drag pressure forces and coefficients by different types of turbulence models and the measured ones by Liu and Graze [7].

TABLE1: COMPARISON OF MEASURED AND COMPUTED LIFT AND DRAG ON STATIONARY CAPSULE IN PIPE

	Lifting force (N)	Lifting coefficient	Drag force (N)	Drag coefficient
Experimental data of Liu and Graze [7]	1.1	0.96	42.5	34.3
Present study a) k-ε	-1.16	-1.01	44.28	35.7
b) k-ω	-3.37	-2.94	45.46	36.7
c) RSM	1.27	1.1	42.36	34.2

From Table 1, it is obvious that both two equations models and the RSM model give a good agreement with the measured value of the drag force with the RSM model having the best agreement. However, for lift prediction, only the RSM model was able to predict the measured value. Table 2 shows comparison of measured and computed Separation zone length (the length from the separation point at the capsule upstream edge to the reattachment point of stream lines. It is clear that the Separation zone length predicted by the RSM gives the nearest value to the measured data.

TABLE2: COMPARISON OF MEASURED AND COMPUTED SEPARATION ZONE LENGTH

Model	k-ε	k-ω	RSM	Measured data of Liddle (Liu and Graze [7]
Separation zone length (cm)	4.38	3.95	7.46	8

By referring to figures 5, 6 and 7, it is clear that in regions of favorable pressure gradient, all the three turbulence models give a trend similar to that of the experimental data. However, in the region of the strongly unfavorable pressure gradient (at the capsule upstream edge) only the RSM model agrees well with the experiments with the two equation models failing to predict the

measured data. This explains why the two equation models (k-ε and k-ω Models) give a negative lifting force as shown in table 1. The reason for that behavior is that as the flow is subjected to a strong variation of pressure gradient or other flow conditions, a different degree of anisotropy is imposed and the process of stress redistribution is affected. Hence, the turbulence field could hardly be simulated by an isotropic eddy diffusivity model (two equations model). Furthermore, by referring to figure 8, it is clear that a separation zone is generated at the capsule upstream edge and the length of this separation is affected by the turbulence model. Moreover, table 2 clearly demonstrates that the results of second moment closure (RSM) model are the nearest values of the predicted separation zone length compared with the measured value.

This separation zone is a laminar zone because it is very close to the wall with low average velocity and predicting the 'by-pass transition from laminar to turbulent' poses different problems. The laminar-to-turbulent transition is promoted by turbulence penetration into the laminar boundary layer from the outer stream with a uniform turbulence field. Savill [25] reviewed the performances of various models in predicting the by-pass transition on a flat plate with different levels of free stream turbulence and revealed that models which do not use the local wall distance in damping functions, perform generally better and that the second-moment closures are generally more powerful than the two-equation models.

Transition on bodies with finite thickness and in non-uniform pressure field involves additional difficulties. Inability to reproduce the proper turbulence level and anisotropy in the stagnation region leads usually to very erroneous results. The illustrative case in figure 8 is the transition in a laminar boundary layer developing over an object (stationary capsule) with sharp edge. Liddle (Liu and Graze [7]) experiments indicate that a laminar separation bubble zone appears at the upstream edge of capsule with length of 8 cm. The transition to turbulence occurs at the rear end of the separation bubble, very close to the wall, followed by a gradual diffusion of turbulence into the outer flow region. Predicting the correct shape and size of the separation region, which is crucial for predicting correctly the transition, requires the application of an advanced turbulence model combined with a very fine numerical grid.

Figure 8 compares computations of the two types of the two equation models and the second-moment closure model (RSM). The two equation models produce the transition and an excessive turbulence level already in the stagnation region as shown in figure 9, causing a strong mixing, which produces a relatively short separation zone. As shown in figure 8, the second-moment closure produces the flow pattern with the nearest value of the laminar separation bubble zone length to that of the measured one. Moreover, the location of the transition and the subsequent development of the turbulence field are in good agreement with experiments. Figure 9 also shows that the RSM model gives many accurate levels of turbulence. The previous discussion provides the limitations of the use of the two equations model in the by pass transition from laminar to turbulent flow.

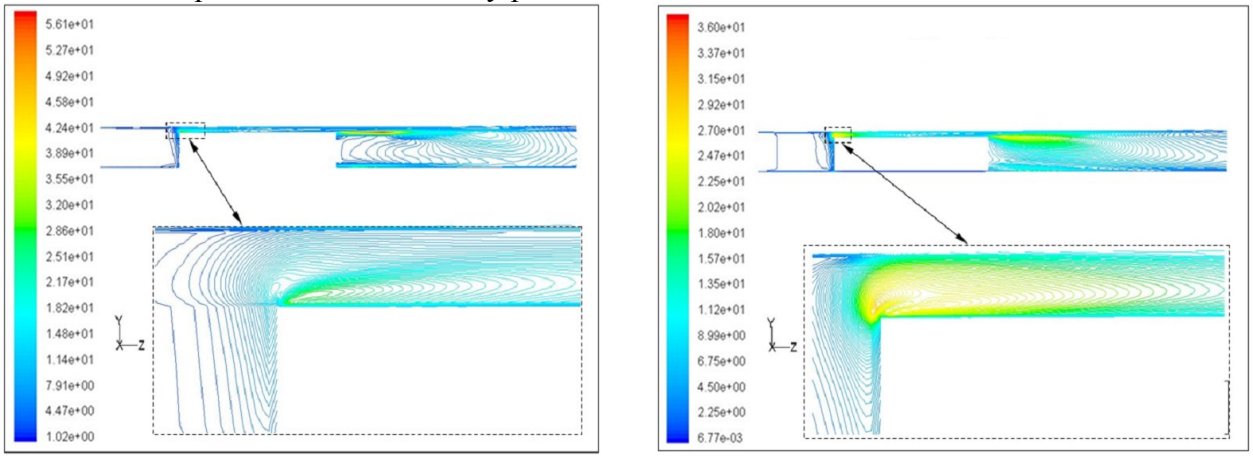

(a) (b)

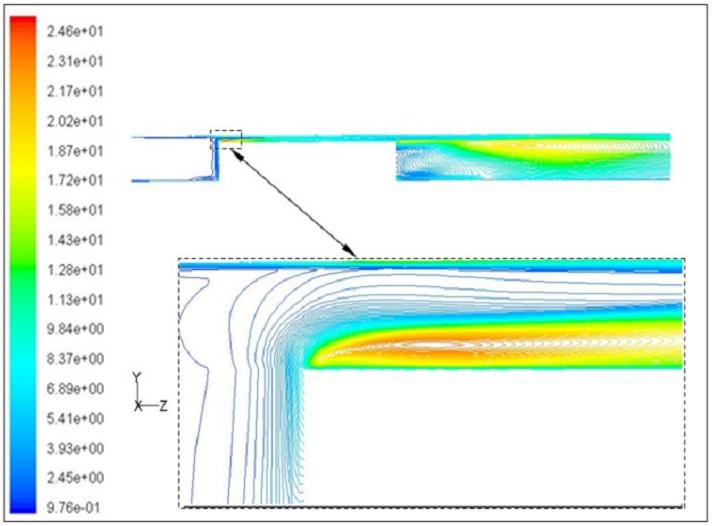

(c)

Figure 9. Turbulence intensity percentage % at the capsule upstream edge, (a) k-ε model, (b) k-ω model, (c) RSM model

4. Conclusion

The present study discussed the flow around a stationary capsule in pipe and provided a model which can be used to simulate the flow around the capsule by predicting the flow stream lines and the pressure distribution not only in the piping part but also across capsule. In addition, the lift and drag on the stationary capsule have been predicted and compared to experimental data. The turbulence models used are two types of two equation models (k-ε and k-ω models) and one type of second moment closure model (RSM model). The following points can be concluded:

1- The two equation models gave a good agreement with the experimental data regarding the pressure distribution and the drag coefficient but failed to predict the lift.
2- The RSM model gave a good agreement with the experiments to predict the pressure distribution, the lift, the drag, and the separation zone length where the second moment closure model gave more accurate turbulence levels (turbulence intensity).
3- When the turbulent flow subjected to strong pressure variation (specially adverse pressure gradient), the isotropic eddy diffusivity model (such as two equation model) has more erroneous results. The strong variation of the pressure gradient or other flow conditions impose a different degree of anisotropy (i.e. the normal stresses are unequal) and affect the process of stress redistribution and turbulence intensities. Consequently, it is concluded that the turbulence field could hardly be simulated by an isotropic eddy diffusivity (such as two equation models).

Nomenclature

C_d	Drag Coefficient.
d_c	Capsule diameter (m).
D	Diameter
K	Turbulence kinetic energy (m^2/s^2).
Kr	Capsule to pipe diameter ratio.
L_c	Capsule length (m).
Re	Reynolds number, $[rV_bd_o/m]$.
S_{ij}	Strain rate (1/s).
S	Capsule specific gravity.

U	Velocity (m/s).
U_t	Friction velocity (m/s).
U^+	Non-dimensional velocity.
y^+	Non-dimensional normal distance from the wall.

Greek

ω	Specific dissipation rate (1/s).
ε	Dissipation rate (m^2/s^3).
ψ	Stream function (kg/s).
ρ	Fluid density (kg/m^3).
μ	Fluid viscosity (Pa/s).
μ_τ	Turbulent eddy viscosity (Pa/s).
θ	Orientation (degrees).
τ_w	The wall shear stress.
ν	Fluid kinematic viscosity (m^2/s)
κ	von Karmen constant.
$-\rho\overline{u_j' u_i'}$	Reynolds stresses (Pa).

References

[1] Liu, H. and Assadollahbaik, M. Energy conservation value of hydraulic container pipeline (HCP). Report No. C00-4935-I. U.S. Dept. of Energy, Washington, D.C. (1979).

[2] Liu, H. and Assadollahbaik, M. Feasibility of using hydraulic capsule pipeline to transport coal. Journal of Pipelines, Vol. 1, (1981). pp. 295-306.

[3] Liu. H. and Wu, J. P. Economic feasibility of using hydraulic pipeline to transport grain in the Midwest of the United States. Freight Pipeline (Proc. 6th Int. Symp, on Freight Pipelines). Hemisphere Publishing Corp., New York. N.Y., (1990). pp. 135-140.

[4] Liu, H. Future freight. , Civ. Engrg., Transactions of the ASCE, Vol. 60, (1990). pp. 78-79.

[5] Govier, G. W., and Aziz, K. The Flow of Capsules in Pipes. The flow complex mixtures in pipes. Van Nostrand-Reinhold, New York, N.Y. (1972).

[6] Liu, H. Hydraulic Capsule Pipeline , Journal of Pipelines, Vol. 1, (1981). pp. 11-23.

[7] Liu, H., and Graze, H. R. Lift and Drag on Stationary Capsule, Journal of Hydraulic Engineering, Transactions of the ASCE, Vol. 109, (1983). pp. 28-47.

[8] Liu, H., and Richards, J. L. Hydraulics of Stationary Capsule in Pipe, Journal of Hydraulic Engineering, Transactions of the ASCE, Vol. 120, (1994). pp. 22-40.

[9] Gao, X. and, Liu, H., Hydraulics Predicting Incipient Velocity of Capsules in Pipe, Journal of Hydraulic Engineering, Transactions of the ASCE, Vol. 126, (2000). pp. 470-473.

[10] Liu, H., The ASCE Task Committee on Freight Pipelines of the Pipeline Division. Freight Pipelines: Current Status and Anticipated Future Use, Journal of Transportation Engineering, Transactions of ASCE, Vol. 124, (1998). pp. 300-310.

[11] Liu, H. Pipeline Engineering , Lewis Publishers, A CRC Press Company, USA. (2003).

[12] Hanjalic, K., Hadzic, I., Jakirlic, S., and Basara, B. Modeling the turbulent wall flows subjected to strong pressure variations, Modeling Complex Turbulent Flows, Kluwer Academic Publishers, Vol. 7, (1999). pp. 203-222.

[13] Huang, P. G. I. Physics and computations of flows with adverse pressure gradients, Modeling Complex Turbulent Flows, Kluwer Academic Publishers, Vol. 7, (1999). pp. 245-258.

[14] Kim, S. E., Choudhury, D., and Patel, B. Computations of Complex Turbulent Flows Using The Commercial Code FLUENT, Modeling Complex Turbulent Flows, Kluwer Academic Publishers, Vol. 7, (1999). pp. 259-276.

[15] Wilcox, D. C. Turbulence Modeling for CFD , Second edition by DCW Industries, Inc., California, USA. (1998).

[16] Ferziger, J. H., and Peric, M. Computational Methods for Fluid Dynamics , Springer-Verlag Berlin Heidelberg New York. (1996).

[17] Khalil, M.F. and Hammoud, A. H. Experimental Investigation of Hydraulic Capsule Pipeline with Drag Reducing Surfactant. , Proc. 8th International Congress of Fluid Dynamics & Propulsion, Sharm El-Sheikh, Sinai, Egypt . 2006.

[18] Khalil, M.F. and Hammoud, A. H. Upward and Downward Inclination of Hydraulic Capsule Pipeline, Proc. 8th International Congress of Fluid Dynamics & Propulsion, Sharm El-Sheikh, Sinai, Egypt . 2006.

[19] Khalil, M.F., Kassab, S.Z., Adam, I.G. and Samaha, M.A. Laminar Flow in Concentric Annulus with a Moving Core, 12th International Water Technology Conference, IWTC12 2008, Alexandria, Egypt, 2008. pp 439-457.

[20] Khalil, M.F., Kassab, S.Z., Adam, I.G. and Samaha, M.A. Turbulent Flow around Single Concentric Long Capsule in a Pipe, Paper No. ICFDP9-EG-209, 9th International Congress of Fluid Dynamics & Propulsion Conference ICFDP 9, ASME, Alexandria, Egypt, Dec. 2008.

[21] Khalil, M.F., Kassab, S.Z., Adam, I.G. and Samaha, M.A. (2008-c), Turbulent Flow around Concentric Capsule Train in Hydraulic Capsule Pipeline (Hcp), 9th International Congress of Fluid Dynamics & Propulsion Conference, ASME, Alexandria, Egypt, Dec. 2008.

[22] Samaha, M. A. Numerical Simulation of the Flow through Hydraulic Capsule Pipeline. MSc Thesis, Faculty of Engineering, Alexandria University, Alexandria 21544, Egypt. 2007.

[23] Launder, B. E. and Spalding, D. B., Lectures in Mathematical Models of Turbulence. Academic Press, London, England, 1972.

[24] Spalding, D. B. Numerical Computation of multi-phase flow and heat transfer, Recent Advances in Numerical Methods in Fluids, Taylor, C. and Morgan, K. (1980).

[25] Savill, A. M. Transition predictions with turbulence models, Transitional Boundary Layers in Aeronautics, North Holland Amsterdam, (1996). pp. 311-319.